

Digital Signal Processing Scheme for Open Loop and Closed Loop IFOG using MATLAB/SIMULINK

G. Harish Babu^{1*}, A. Venkata Anuhya² and N. Venkatram³

¹Department of ECE, Aurora's Scientific & Technological Institute, Hyderabad - 501301, Telangana, India; harish.sidhu12@gmail.com

²Department of ECE, St.Mary's Women's Engineering College, Guntur - 522017, Andhra Pradesh, India; anuhya409@gmail.com

³Department of ECM, K L University, Guntur - 522502, Andhra Pradesh, India; venkatram@kluniversity.in

Abstract:

Objective: Interferometric Fiber optic gyroscope (IFOG) is an angular rate sensor which plays a crucial role in inertial navigation system. Measuring the angular rotation rate can be done in two approaches namely open loop & closed loop. Designing and implementation of these methods using a simulation tool provides faster & accurate results. This paper presents a novel Simulink model implementation of Open loop & Closed loop Fiber optic gyroscope for the measurement of rotation rate. **Method/Analysis:** The gyroscope with each optical component is treated as a black box having M input and N output ports that are represented mathematically with its transfer function by connecting output to its input. This methodology is very efficient for finding the calibration & phase difference between the co-rotating & counter rotating beams. **Findings:** There are two major contributions in this paper. Firstly, the physical model of open loop FOG is built in Simulink model & angular rate is measured. The signal processing scheme of modulation and demodulation techniques for finding the rotation rate can also be analyzed mathematically. In second, to improve the accuracy and stability the feedback loop is very important to improve the gyro performance which can also be analyzed with different rotation rates. Experimental setup shows that an improved result is obtained in determining the direction of rotation and accuracy of the proposed model.

Keywords: Black Box, Closed Loop, Interferometric Fiber Optic Gyroscope (IFOG), Open Loop, Simulation, Simulink Model, Transfer Function

1. Introduction

Many exciting developments have taken place especially in the area of inertial navigation sensors¹. Estimation of precise speed is valuable in various applications²; from rocket route to movement control³. Sensitivity, resolution, and stability, time are the primary performance measures of gyroscopes. Micro Electro Mechanical System (MEMS) gyroscopes⁴ which was used earlier in Inertial Navigation System (INS) was less reliable, sensitivity, less dynamic

range, large moving parts, complexity, large bandwidth and takes more reaction time. Recent advances in technology motivated researchers for the development of optical gyros such as Ring Laser Gyroscope (RLG) and fiber optics gyroscope (FOG) whose became the conventional counterparts to MEMS gyros. Optical fibers have been intensively investigated at various sensor fields because of their unique characteristics such as multiplexing, remote sensing, high flexibility, low propagating loss, high sensitivity, low fabrication cost, small form factor, high accuracy, simul-

*Author for correspondence

taneous sensing ability, and immunity to electromagnetic interference. Moreover, RLG technology⁵ is also complex because of its large size, weight, cost, less accuracy and consumption of large power. Fiber optic technology has a great support from two growing fields namely optical communication and silicon technology plays a vital role for the development of fiber optic gyroscope. Fiber Optic Gyroscope (FOG) has been used for measuring the rotation angle. FOGs were developed in the 1980s as a more compact, albeit less sensitive, alternative to RLGs.

Fiber optic gyroscope uses two beams of light which propagate simultaneously around a path of optical fiber to measure angular velocity⁶. The rotation of the plane in which the optical fiber lies induces a phase difference between the two waves which is proportional to the angular velocity of the rotation. This phenomenon is known as Sagnac effect⁷. The optical waves fall onto a photoelectric sensor which produces a current dependent on the intensity of the light waves.

One important advantage of the FOG is its ruggedness. It contains no moving parts unlike other competitors such as mechanical gyroscopes and ring laser gyroscopes (dithering is involved in ring laser gyroscopes). Due to these unique advantages, it seems likely that the FOG will play a significant role in both military and commercial markets⁸. Recently, FOG is being widely used in defence applications, due to its small size, low cost, light weight, large dynamic range, low power consumption, and possible batch fabrication.

FOG is configured in two ways as resonator fiber optic gyroscope (RFOG)⁹ and Interferometric Fiber Optic Gyroscope (IFOG). RFOG is similar to RLG, and its usage is less in applications because of limited performance. The signal processing of FOG is carried out in two approaches

such as open loop and closed loop. Open loop approach is less sensitive because of amplitude¹⁰ and returning optical power variations at the phase modulator which in turn causes non-linearity behavior and scale factor instability in the FOG output. Improvements in sensitivity, linearity and dynamic range can be realized by using a "closed-loop" configuration. In closed loop approach, the non-reciprocal phase shift between two counter propagating light beams is induced to counterbalance the rotation induced sagnac phase shift error¹¹. These fiber gyros have the wide dynamic range and high linearity needed to support stringent navigation requirements.

1.1. Problem Definition

Implementation of open loop FOG in simulink model is yet simple, provides a good accuracy and improves a dynamic range which almost meets the closed loop specifications. Designing in simulink¹² software takes less time to operate, low cost and provides good results. The implementation of Open loop and closed loop configurations in simulink model is different and results are compared with each other.

2. Modulation and Demodulation of Open Loop and Closed Loop IFOG

2.1. Open Loop Configuration

The scheme of open loop approach is similar to sagnac interferometer. The block diagram is shown in Figure 1.

FOG is configured with a light source, such as a super luminescent diode (SLD), is projected into a 3-dB

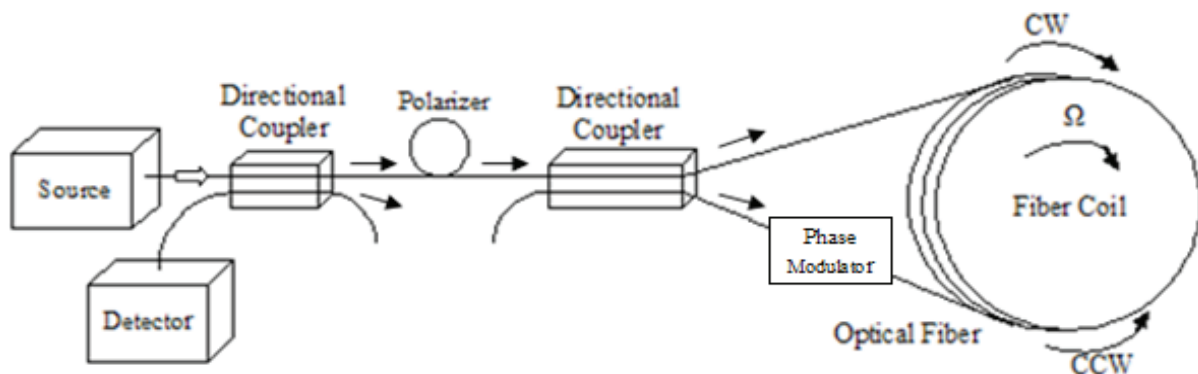


Figure 1. Block diagram of open loop fiber optic gyroscope.

fiber optic coupler that splits the light into two waves. After traversing the coupler, the two light waves pass through a polarizer and reaches the 2nd coupler. The problem of reciprocity is overcome by the introduction of 2nd coupler.

Later the two waves propagate through a medium equally in opposite directions around the fiber optic coil. The light waves interfere upon return to coupler and project a fringe pattern onto a photo-detector. In accordance with any two-wave interferometer, the intensity on the photo detector, which represents a mixture of the two light waves, varies as cosine of Sagnac phase with its maximum value at zero as shown in Figure. This intensity is expressed as,

$$I = I_0(1 + \cos(\Delta\phi_s))$$

where, I_0 is the mean value of the intensity.

The detected intensity is used to calculate the rotation rate. In the case of no rotation $\Delta\phi_s = 0$, the light waves will combine in phase, which results in maximum intensity. When the open loop approach is subjected to sinusoidal modulation, the signal processing of open loop is as discussed below.

2.1.1. Modulation

Standard bias modulation technique is,

$$\phi_m(t) = \phi_0 \sin(\omega_m t)$$

So $\Delta\phi_m(t)$ becomes

$$\Delta\phi_m(t) = \phi_0 \sin(\omega_m t) - \phi_0 \sin(\omega_m t - \omega_m \tau)$$

Using trigonometric identity: $\sin A - \sin B = 2 \cos((A+B)/2) \sin((A-B)/2)$

$$\Delta\phi_m(t) = 2\phi_0 \cos(\omega_m t - \omega_m \tau / 2) \sin(\omega_m \tau / 2)$$

Defining constants to simplify: $\delta = \omega_m \tau / 2$, and $\alpha = 2\phi_0 \sin(\delta)$

$$\Delta\phi_m(t) = \alpha \cos(\omega_m t - \delta)$$

$$I = \frac{I_0}{2} [(1 + \cos \Delta\phi_s(t) + \Delta\phi_s(t))]$$

$$= \frac{I_0}{2} \left[1 + (\cos \Delta\phi_s(t) \cos \Delta\phi_m(t) - \sin \Delta\phi_s(t) \sin \Delta\phi_m(t)) \right]$$

The harmonic contents of this signal is to be found using Bessel function identities.

$$\cos(x \sin \theta) = J_0(x) - 2J_2(x) \cos 2\theta + 2J_4(x) \cos 4\theta - \dots$$

$$\sin(x \sin \theta) = 2J_1(x) \sin \theta - 2J_3(x) \cos 3\theta + 2J_5(x) \cos 5\theta + \dots$$

Detector current can be expressed in terms of Bessel's function 'J' as,

$$I_d = I_0 [1 + [J_0(\phi_m) + 2 \sum_{k=1}^{\infty} J_{2k}(\phi_m) \cos 2k\omega_m t] \cos(\Delta\phi_s) + [2 \sum_{k=1}^{\infty} J_{2k-1}(\phi_m) \sin(2k-1)\omega_m t] \sin(\Delta\phi_s)]$$

The photo detected signal contains, in addition to a DC component, all the harmonics of the modulating signal.

From the Bessel identities above, it can be seen that

- $[\sin(\Delta\phi_m(t))]$ terms give odd harmonics of
- $[\cos(\Delta\phi_m(t))]$ terms give odd harmonics of

2.1.2. Demodulation

The frequency content of the detector signal can be obtained by synchronously demodulating with 'sine' and 'cosine' functions, and is possible to extract the rotation rate.

$$I_d = I_0 [1 + [J_0(\phi_m) + 2 \sum_{k=1}^{\infty} J_{2k}(\phi_m) \cos 2k\omega_m t] \cos(\Delta\phi_s) + [2 \sum_{k=1}^{\infty} J_{2k-1}(\phi_m) \sin(2k-1)\omega_m t] \sin(\Delta\phi_s)]$$

By expanding the summation equation, we get,

$$I_d = I_0 [1 + [J_0(\phi_m) \cos(\Delta\phi_s) - 2J_1(\phi_m) \sin(\Delta\phi_s) \sin \omega_m t + 2J_2(\phi_m) \cos 2\omega_m t \cos(\Delta\phi_s) - 2J_3(\phi_m) \sin(\Delta\phi_s) \sin 3\omega_m t + 2J_4(\phi_m) \cos 4\omega_m t \cos(\Delta\phi_s) - \dots]$$

Multiplying with "Sin $\omega_m t$ " on both sides we get

$$I_d(\sin \omega_m t) = I_0 (\sin \omega_m t) + [I_0 J_0(\phi_m) \cos(\Delta\phi_s) (\sin \omega_m t) - 2J_1(\phi_m) \sin(\Delta\phi_s) I_0 \sin^2 \omega_m t + \dots 2J_2(\phi_m) I_0 \sin \omega_m t \cos 2\omega_m t \cos(\Delta\phi_s) - 2J_3(\phi_m) I_0 \sin(\Delta\phi_s) (\sin \omega_m t) \sin 3\omega_m t + 2J_4(\phi_m) \cos 4\omega_m t \cos(\Delta\phi_s) - \dots]$$

$$\begin{aligned}
 I_d(\sin \omega_m t) &= I_0(\sin \omega_m t) + I_0 J_0(\phi_m) \cos(\Delta \phi_s)(\sin \omega_m t) \\
 &\quad - 2J_1(\phi_m) \sin(\Delta \phi_s) I_0[(1 - \cos 2\omega_m t)/2] \\
 &\quad + 2J_2(\phi_m) I_0 \sin \omega_m t \cos 2\omega_m t \cos(\Delta \phi_s) \\
 &\quad - 2J_3(\phi_m) I_0 \sin(\Delta \phi_s)(\sin \omega_m t) \sin 3\omega_m t \\
 &\quad + 2J_4(\phi_m) I_0(\sin \omega_m t) \cos 4\omega_m t \cos(\Delta \phi_s) - \dots
 \end{aligned}$$

$$\begin{aligned}
 I_d(\sin \omega_m t) &= I_0(\sin \omega_m t) + I_0 J_0(\phi_m) \cos(\Delta \phi_s)(\sin \omega_m t) \\
 &\quad - J_1(\phi_m) \sin(\Delta \phi_s) I_0 + J_1(\phi_m) \sin(\Delta \phi_s) I_0 \cos 2\omega_m t \\
 &\quad + 2J_2(\phi_m) I_0 \sin \omega_m t \cos 2\omega_m t \cos(\Delta \phi_s) \\
 &\quad - 2J_3(\phi_m) I_0 \sin(\Delta \phi_s)(\sin \omega_m t) \sin 3\omega_m t \\
 &\quad + 2J_4(\phi_m) I_0(\sin \omega_m t) \cos 4\omega_m t \cos(\Delta \phi_s) - \dots
 \end{aligned}$$

Considering the cut of frequency as ' $f_m/2$ ', assume $I_d(\sin \omega_m t) = I_1$ and is passed through LPE, the equation becomes

$$I_1 = I_0[-J_1(\phi_m) \sin(\Delta \phi_s)]$$

$$I_1 / I_0 = -J_1(\phi_m) \sin(\Delta \phi_s)$$

$$\sin(\Delta \phi_s) = -I_1 / (I_0 J_1(\phi_m))$$

$$\Delta \phi_s = -\sin^{-1}[-I_1 / (I_0 J_1(\phi_m))]$$

When multiplying the detector current equation with ' $\cos 2\omega_m t$ ' assume $I_d(\cos 2\omega_m t) = I_2$ and is passed through LPE, the equation becomes

$$I_2 = I_0[J_2(\phi_m) \cos(\Delta \phi_s)]$$

$$I_2 / I_0 = J_2(\phi_m) \cos(\Delta \phi_s)$$

$$\cos(\Delta \phi_s) = I_2 / (I_0 J_2(\phi_m))$$

$$\Delta \phi_s = \cos^{-1}[I_2 / (I_0 J_2(\phi_m))]$$

Also take, $I_d(\sin 3\omega_m t) = I_3$ and $I_d(\cos 4\omega_m t) = I_4$, the above process repeats therefore we get,

$I_1 = I_0[-J_1(\phi_m) \sin(\Delta \phi_s)]$	1 st harmonic
$I_2 = I_0[J_2(\phi_m) \cos(\Delta \phi_s)]$	2 nd harmonic
$I_3 = I_0[-J_3(\phi_m) \sin(\Delta \phi_s)]$	3 rd harmonic
$I_4 = I_0[J_4(\phi_m) \cos(\Delta \phi_s)]$	4 th harmonic & so on...

By taking the I_2 / I_4 and I_1 / I_2 ,

$$I_2 / I_4 = J_2(\phi_m) / J_4(\phi_m)$$

$$I_2 / I_4 = [J_1(\phi_m) / J_2(\phi_m)] \tan(\Delta \phi_s)$$

The sagnac phase error can be taken as,

$$\Delta \phi_s = \tan^{-1}[J_1(\phi_m) I_1 / J_2(\phi_m) I_2]$$

From the above equation we are getting the sagnac phase shift. In order to get the given input rotation rate from the above equation,

$$\Delta \phi_s = \frac{2\pi LD}{\lambda C} * \Omega$$

Thus the demodulation is done and the rotation rate is calculated from it.

Detector signal contains all harmonics of ω_m but desirable part is at 1st harmonic of ω_m . In order to extract signal at ω_m only, Lock-in Amplifier (LIA) can be used.

- If $\Delta = 0$, $\Delta \phi_s = 0$ signal vanishes.
- For $\Delta \phi_s \ll 1$, signal $\approx \sin \Delta \phi_s \approx \Delta \phi_s$
- Signal polarity reverses when rotation direction switches. $\Delta \phi_s$ to $-\Delta \phi_s$
- Comparing to un-modulated signal;
- Un-modulated for signal $\approx (1 + \cos \Delta \phi_s) \approx \Delta \phi_s^2$
- Sign of un-modulated signal independent of rotation direction.

2.2. Closed Loop Configuration

The basic configuration of closed loop approach is shown in Figure 2,

A feedback loop is added to the open loop configuration. The amplifier output is given to A/D converter which samples and quantizes the output and performs a synchronous demodulation and is given to the controller to extract the phase error. The corresponding sampling frequency is inverse of the radiation transit time τ , for the required synchronization of the ramp and the biasing signal.

The filtering and amplification process is done in controller. If the filtering and amplification are properly adjusted, then the feedback loop will provide a non-reciprocal phase shift that is always nearly equal and opposite in sign to the Sagnac phase for all constant input rotation rates.

$$\phi_f = -\Delta \phi_s$$

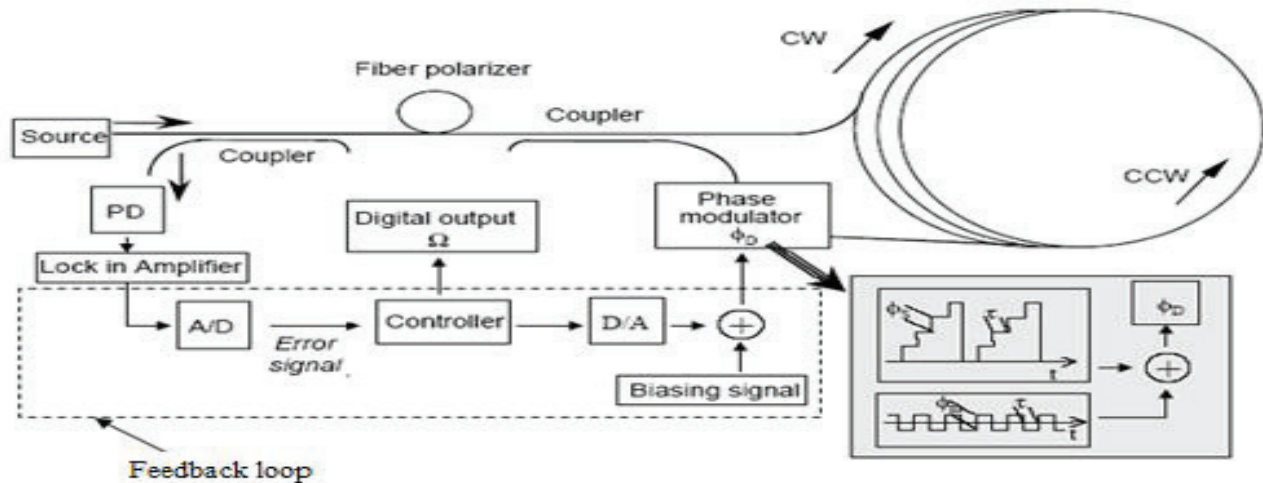


Figure 2. Block diagram of closed loop fiber optic gyroscope.

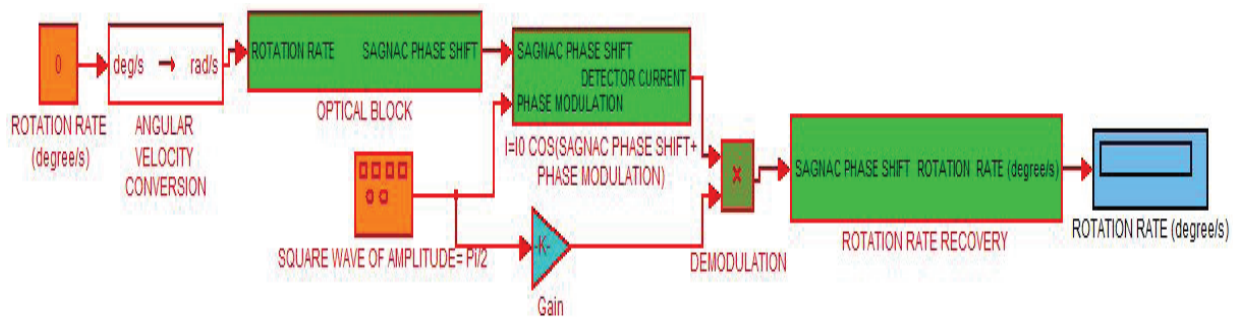


Figure 3. Simulink model of open loop fiber optic gyroscope.

The feedback loop generates a staircase ramp signal whose slope is proportional to the rotation rate ' Ω '. The duration of each digital step is normally equal to coil transit time τ and step height is equal to sagnac phase. This modulation technique is called a digital serrodyne technique. The amplitude of the ramp signal is equal to the 2π voltage¹³ of the IOC (Integrated Optic Chip). The amplitude of the square wave is $V \pi/2$ of IOC.

3. Proposed Method

Among the considerations of simplicity, low cost, flexibility, durability, less execution time, high accuracy, and stability the open loop and closed loop configurations are designed in simulink model.

3.1. Open Loop Design using Simulink

The open loop configuration of FOG is designed in simulink is as shown in Figure 3.

The implementation of open loop structure in simulink model is similar to the basic configuration but slightly different in design. The configuration consists of several modules, each treated as a block box, with its corresponding inputs and outputs. The design of such model in simulink is simple, reliable and low cost. The model of this system also acts as checking tool to extract the required rotation rate information.

The input to the system is the rotation rate which was given in terms of degree/sec. The angular velocity conversion block converts degree/sec into radians/

sec information. The output is given to the optical module. The optical block is designed with the help of gyro specifications such as length of the fiber coil, diameter, wavelength and velocity of light, which generates the amount of sagnac phase shift involved in the block with respect to the given input rotation rate. The phase modulator undergoes a square wave modulation whose amplitude is $\pi/2$ volts. Square wave modulation is used to modulate the light thereby increase the sensitivity and direction of rotation.

The sagnac phase between two counter propagating waves and the phase modulator output are combined using an internal adder in place of coupler and reaches the detector. That adder output is given as input to the detector photo detector. Then the corresponding detector current output is obtained using trigonometric functions like 'cos', i.e. the detector current is the function of sagnac phase and standard modulation technique.

$$I = I_0[1 + \cos(\Delta\phi_s(t) + \Delta\phi_m(t))]$$

The result is also known as square wave modulated co-sinusoidal signal which is also known as phase error signal. The output of the photo detector is synchronously demodulated by using a reference square wave signal in order to extract the sagnac phase error present in the system.

The sagnac phase error contains the rotation rate information and it is extracted using the formula,

$$\phi_s = \frac{2\pi LD \Omega}{\lambda C}$$

where,

L = Length of fiber.

λ = Wavelength of light.

C = Velocity of light.

Ω = Rotation rate.

D = Diameter of fiber coil.

The process of extracting the rotation rate from sagnac phase error is done in rotation recovery process. The output is the amount of rotation that a designed model can sense.

3.2. Closed Loop Design using Simulink Model

The design of closed loop configuration is shown in Figure 4.

In closed loop configuration, feedback unit is added to the open loop approach. The feedback control unit provides a non-reciprocal phase shift which is equal in magnitude but opposite in sign to nullify the rotation induced sagnac error. The feedback loop acts as data acquisition and signal processing unit to achieve the closed loop operation. it generates a phase nullifying signal and bias to the phase modulator of the FOG.

It accepts the modulated sagnac phase error signal from photo detector of gyro and demodulated synchronously with the help of reference square wave whose

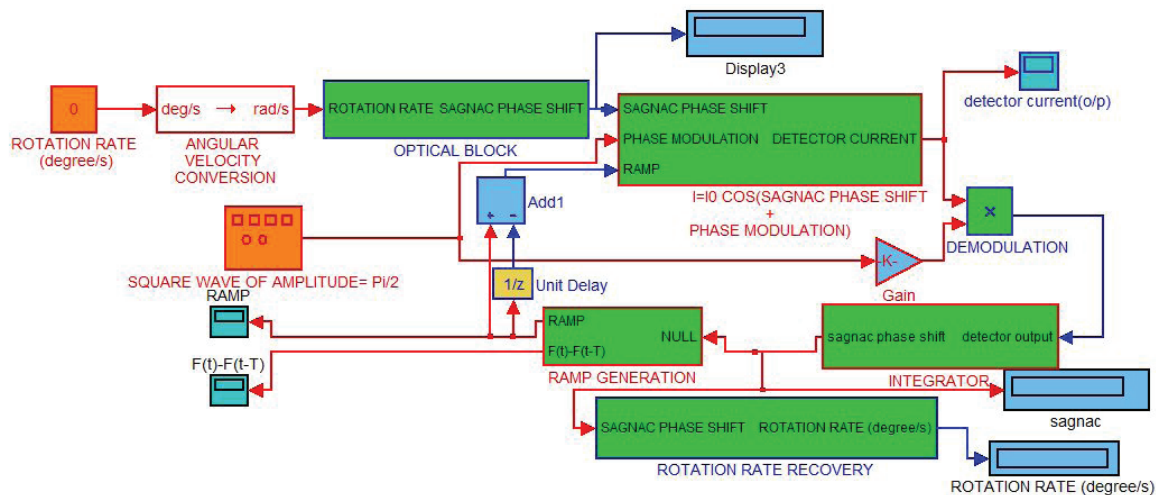


Figure 4. Simulink model of closed loop fiber optic gyroscope.

amplitude is $\pi/2$ volts of optic chip. This is used to get maximum sensitivity at lower rotation rates. The demodulator output is given to the integrator module. The integrator integrates the signal with respect to coil transit time and generates a dc value. The dc value must be adjusted equally to the sagnac phase value with some gain 'k'. The output of integrator is used to generate the staircase feedback phase nullifying signal i.e. ramp signal by using upper and lower threshold limits.

As the gyro detector current is a 'cosine' dependent function, the amplitude of ramp is reset to 2π . The reset step corresponds to a phase variation of 2π radian, in order to get always the correct Sagnac phase shift. The ramp signal and delayed ramp signal are differentiated to get the differential pulse signal. That differential pulse represents is the phase nullifying signal given as feedback

to the phase modulator. Therefore, the detector current can be expressed as,

$$I = I_0 [1 + \cos(\Delta\phi_s(t) + \Delta\phi_m(t) - \Delta\phi_{fb})]$$

where, is the feedback phase used to counteract the phase error.

Again the output of the detector is demodulated and integrates the signal to extract the rotation rate information. The integrated output is converted into rotation rate through sagnac formula.

4. Results and Discussion

4.1. Open Loop Results

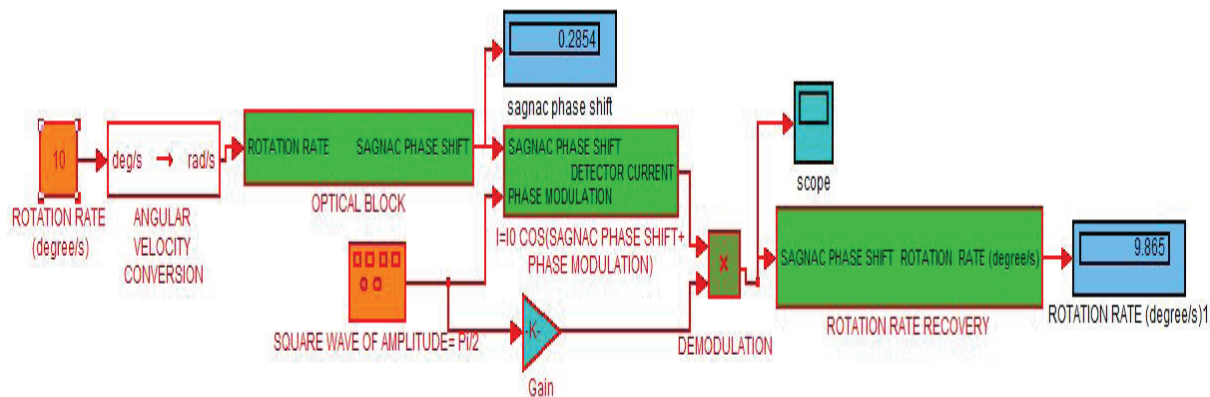


Figure 5. Open loop FOG output when input rotation is 10o/sec.

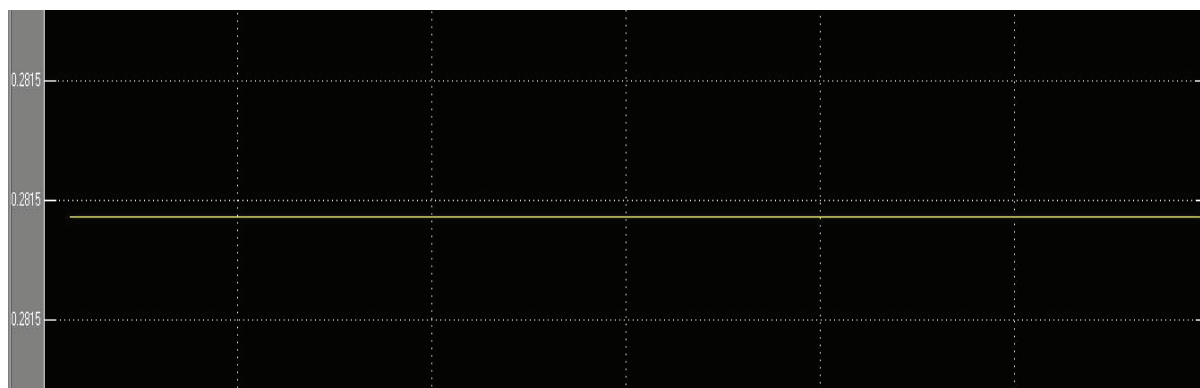


Figure 6. The amount of sagnac phase present in Open loop FOG when input rotation is 10o/sec.

4.2. Closed Loop Results

In the differential pulse, the constant indicates the given input rotation rate while the pulse peak end represents the reset value of ramp.

5. Conclusion

In this paper, a simple and fast simulation tool using simulink model has been developed for designing the open loop and closed loop fiber optic gyroscope. The

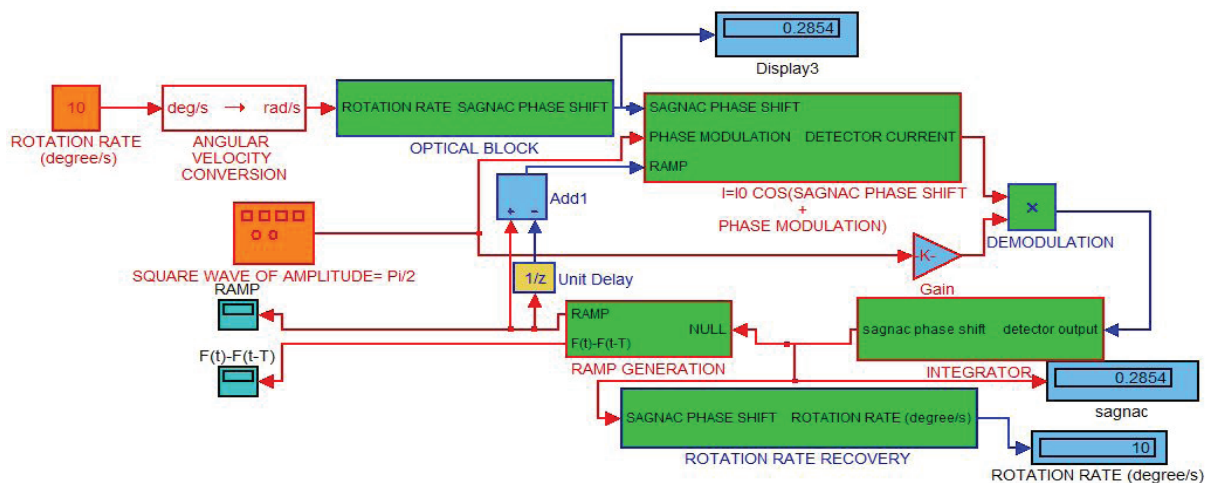


Figure 7. Simulink model of closed loop fiber optic gyroscope when input rotation rate is 10o/sec.

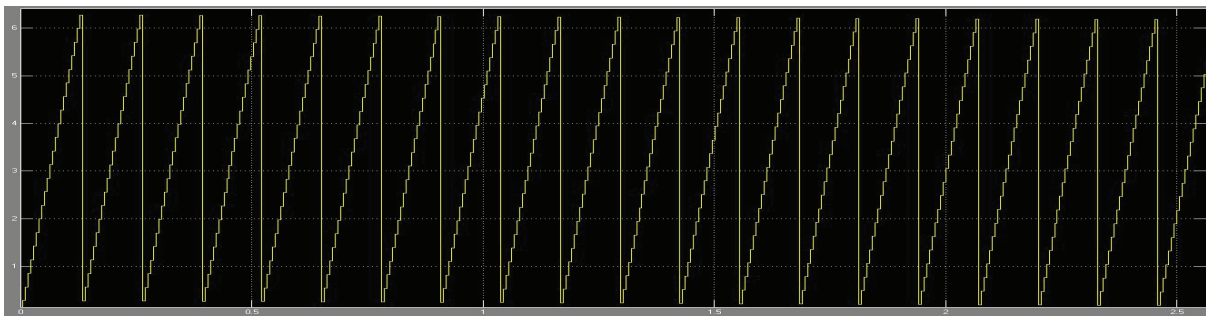


Figure 8. Positive going ramp when the given input rotation rate is positive.

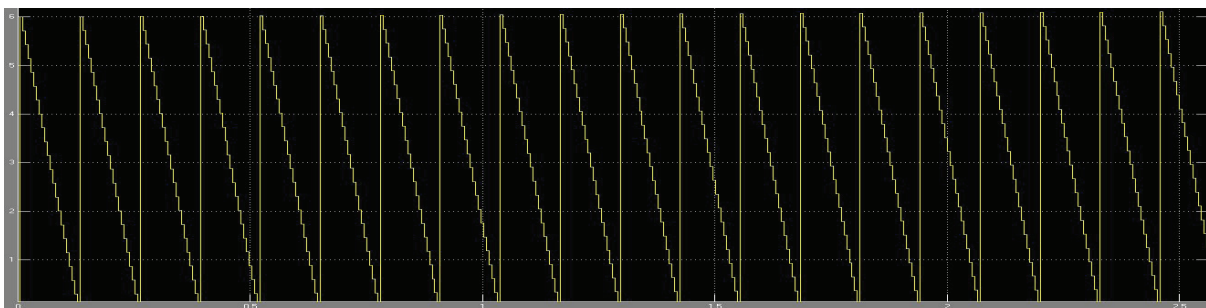


Figure 9. Negative going ramp when the given input rotation rate is negative.

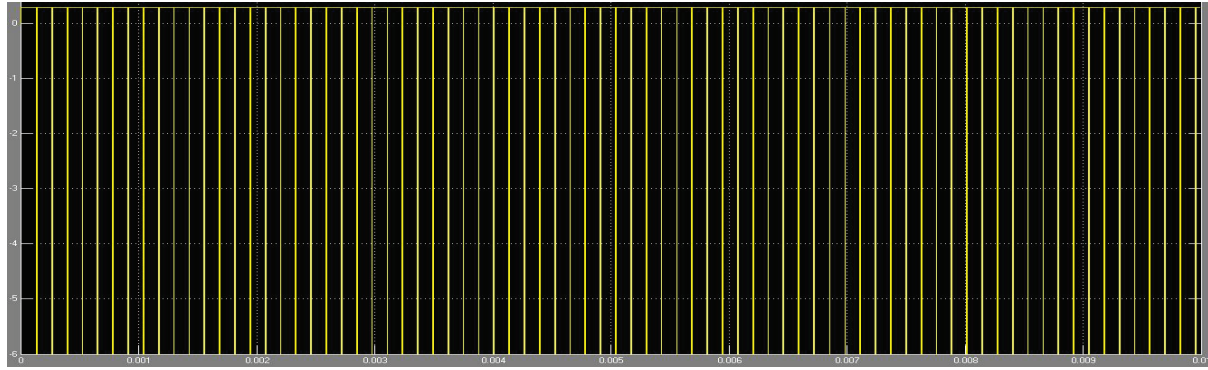


Figure 10. Differential pulse when the given input rotation rate is positive.

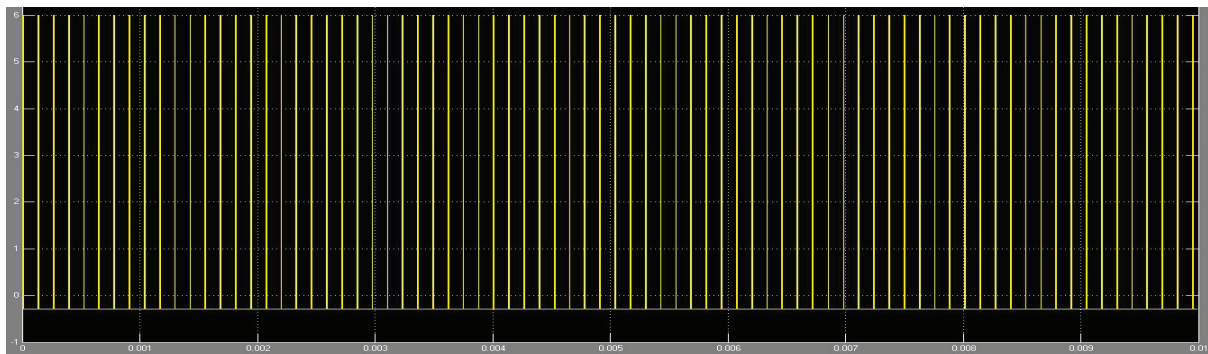


Figure 11. Differential pulse when the given input rotation rate is negative.

proposed method works well for easily understanding the operation, designing of FOG unit, and its functionality and rotation rate recovery. This model requires a minimum number of essential optical components for designing the FOG. Further developments are needed to implement this model in real time under different environmental conditions.

6. References

1. Merlo S, Norgia M, Donati S. Fiber gyroscope principles. Electro optics Group, University of Pavia, Italy, Handbook of Fibre Optic Sensing Technology, edited by José Miguel López-Higuera, John Wiley & Sons Ltd; 2000.
2. Karthik S. UnderWater vehicle for surveillance with navigation and swarm network communication. Indian Journal of Science and Technology. 2014 Oct; 7(S6):22–31. doi: 10.17485/ijst/2014/v7iS6/54589.
3. Fidanboyu K, Efendioglu HS. Fiber optic sensors and their applications. 5th International Advanced Technologies Symposium (IATS'09); Karabuk: Turkey; 2009 May 13–15. p.1–6.
4. Sternberg H. HafenCity University Hamburg. Qualification Process for MEMS Gyroscopes for the use in Navigation Systems; HafenCity University Hamburg; 2011 Oct. p.1–8.
5. Juang JN. Evaluation of ring laser and fiber optic gyroscope technology school of engineering. Mercer University; Macon, GA 31207: USA.
6. Kumar UR, Khanna V, Saravanan T. Chromatic dispersion compensation in optical fiber communication system and its simulation. Indian Journal of Science and Technology. 2013 May; 6(6S):4762–66. doi: 10.17485/ijst/2013/v6i6/33959.
7. Kim BY, Park M, Calif. Interferometric sensor using time domain measurements; US; 1988 Oct 25. p.1–8.
8. Lee B. Review of the present status of optical fiber sensors. Optical Fiber Technology. 2003; 9(2):57–79.
9. Merlo S, Norgia M, Donati S. Fiber gyroscope principles. Electro optics Group; University of Pavia: Italy; 2000.
10. Gronau Y, Tur M. Digital signal processing for an open loop fiber optic gyroscope. Applied Optics. 1995 Sep 1; 34(25):5849–53.

11. Khan MH. Open-loop fiber-optic gyroscope. A Technical Note. Hindustan Aeronautics Limited. Korwa, and C. Ramakrishna. Institute of Armament Technology, Pune - 411 025, Defence Science Journal. 1996 Oct; 46(4):283–8.
12. Rajulapati RM, Nayak J, Scientist(F). Modeling and simulation of signal processing for a closed loop fiber optic gyro's using FPGA. International Journal of Engineering Science & Technology. 2012 Mar, 4(3):947–59.
13. Sireesha T, Ravi KS. Comparative assessment on ramp and bias voltage variations of closed loop interferometric fiber optic gyroscope. Indian Journal of Science and Technology. 2015 Oct 9; 8(18):27–37. doi: 10.17485/ijst/2015/v8i18/67723.